Cytotherapy 22 (2020) 762–771

Contents lists available at ScienceDirect

CYTOTHERAPY

journal homepage: www.isct-cytotherapy.org

International Society ISCT Cell & Gene Therapy®

FULL-LENGTH ARTICLE

Manufacturing

Pancreas-derived mesenchymal stromal cells share immune response-modulating and angiogenic potential with bone marrow mesenchymal stromal cells and can be grown to therapeutic scale under Good Manufacturing Practice conditions

Kayleigh L. Thirlwell[1,2], David Colligan[1], Joanne C. Mountford[1], Kay Samuel[1], Laura Bailey[1], Nerea Cuesta-Gomez[2], Kay D. Hewit[1,2], Christopher J Kelly[2], Christopher C. West[3], Neil W.A. McGowan[1], John J. Casey[5], Gerard J. Graham[2], Marc L. Turner[1], Shareen Forbes[4,5], John D.M. Campbell, PhD[1,2,*]

[1] *Tissues, Cells and Advanced Therapeutics, The Jack Copland Centre, Scottish National Blood Transfusion Service, Edinburgh, UK*
[2] *Chemokine Research Group, Institute of Infection, Immunity and Inflammation, University of Glasgow, Glasgow, UK*
[3] *Department of Surgery, University of Edinburgh, Edinburgh, UK*
[4] *University/British Heart Foundation Centre for Cardiovascular Science, Queens Medical Research Institute, University of Edinburgh, Edinburgh, UK*
[5] *Transplant Unit, National Islet Transplant Programme, Royal Infirmary of Edinburgh, Edinburgh, UK*

ARTICLE INFO

Article History:
Received 9 September 2019
Accepted 17 July 2020

Key Words:
chemokines
Good Manufacturing Practice
mesenchymal stromal cells
pancreatic islet
T-cell suppression
xenogeneic-free

ABSTRACT

Background aims: Mesenchymal stromal cells (MSCs) isolated from various tissues are under investigation as cellular therapeutics in a wide range of diseases. It is appreciated that the basic biological functions of MSCs vary depending on tissue source. However, in-depth comparative analyses between MSCs isolated from different tissue sources under Good Manufacturing Practice (GMP) conditions are lacking. Human clinical-grade low-purity islet (LPI) fractions are generated as a byproduct of islet isolation for transplantation. MSC isolates were derived from LPI fractions with the aim of performing a systematic, standardized comparative analysis of these cells with clinically relevant bone marrow-derived MSCs (BM MSCs).
Methods: MSC isolates were derived from LPI fractions and expanded in platelet lysate-supplemented medium or in commercially available xenogeneic-free medium. Doubling rate, phenotype, differentiation potential, gene expression, protein production and immunomodulatory capacity of LPIs were compared with those of BM MSCs.
Results: MSCs can be readily derived *in vitro* from non-transplanted fractions resulting from islet cell processing (i.e., LPI MSCs). LPI MSCs grow stably in serum-free or platelet lysate-supplemented media and demonstrate *in vitro* self-renewal, as measured by colony-forming unit assay. LPI MSCs express patterns of chemokines and pro-regenerative factors similar to those of BM MSCs and, importantly, are equally able to attract immune cells *in vitro* and *in vivo* and suppress T-cell proliferation *in vitro*. Additionally, LPI MSCs can be expanded to therapeutically relevant doses at low passage under GMP conditions.
Conclusions: LPI MSCs represent an alternative source of GMP MSCs with functions comparable to BM MSCs.

Introduction

Mesenchymal stromal cells (MSCs) are multipotent cells found in variable numbers in the majority of tissues. Their immunoregulatory, pro-regenerative and differentiation potential, coupled with their relative ease of procurement, has made them attractive as cellular therapeutics [1]. Currently, there are over 1300 registered clinical trials

* Correspondence: Professor John D.M. Campbell PhD FRSB, Tissues, Cells and Advanced Therapeutics, The Jack Copland Centre, Scottish National Blood Transfusion Service, 52 Research Avenue North, Edinburgh, UK.
E-mail address: johncampbell3@nhs.net (J.D.M. Campbell).

https://doi.org/10.1016/j.jcyt.2020.07.010

using MSCs isolated from a variety of tissues in a wide range of disease and transplant settings [2]. Historically, the majority of the clinical data has been generated using bone marrow-derived MSCs (BM MSCs); therefore, much of the understanding of MSC function relates to BM cells. Although living donor bone marrow donation is well established, bone marrow aspirates contain relatively low numbers of MSCs that require extensive expansion to reach therapeutic doses [3], and the ease of generating therapeutically relevant doses of functional MSCs reduces with increasing donor age [4,5]. BM MSCs expanded at a large scale show a degree of phenotypic and functional variation over time [6]. These passage-dependent functional and phenotypical changes may underlie an observed decline in *in vivo* function; for example, BM MSCs are more efficacious when used at lower passage in patients with graft-versus-host disease (GVHD) [7]. As a result, BM MSCs may not be ideal for every therapeutic situation; therefore, there has been a concerted effort to look for alternative tissue sources, including adipose tissue and umbilical cord [8–10]. MSCs isolated from different sources are not identical in their biological function, with differences including immunosuppressive ability and angiogenic potential [11–14]. This is extremely important to keep in mind when considering MSC therapeutic capacity [14],

When contemplating MSC therapeutic modes of action, it is likely that MSC anti-inflammatory function works in concert with MSC tissue-building capacity. These functions are elaborated in part by chemokines, which are vital in attracting immune cells, such as monocytes (CCL2) and neutrophils (CXCL2) [13]; immune-modulating factors, such as prostaglandin E2 [15] and indolamine 2,3-dioxygenase (IDO) [16]; and a variety of angiogenic factors, including vascular endothelial growth factor and CXCL8 [14]. These properties are amplified by licensing with various stimulatory factors, including interferon gamma, tumor necrosis factor alpha and IL-1β. Response to these cytokines can be variable depending on the tissue source [17–19]. The authors recently conducted a comparative analysis of adipose- and umbilical cord-derived MSCs for differential expression of a suite of chemokines and immune-modulating and angiogenic factors [14]. Anti-inflammatory and pro-angiogenic phenotypes correlated with positive outcomes in a transplant model [14]. These methods are yet to be applied to MSCs derived from other tissues.

Pancreatic-derived MSCs have been described by a number of groups [19,20]. They can be isolated from waste products of pancreatic islet transplantation. Islet transplantation is used to treat individuals with type 1 diabetes mellitus with unstable glycemic control [21,22]. It is an efficacious treatment involving enzymatic dissociation of donor pancreata under Good Manufacturing Practice (GMP) conditions to release islets for transplantation [22]. Highly pure islets are transplanted into recipients, leaving a fractionated byproduct of digested exocrine tissue and low-purity islets (LPIs)—small numbers of islets plus attached exocrine tissue. In this study, the authors investigated the potential of using the LPI fraction as starting material for GMP-compliant manufacture of MSC. The authors determined that LPI material can be used to manufacture MSCs under GMP conditions at scale. LPI MSCs expanded using GMP-compatible reagents were systematically evaluated for their pro-regenerative and inflammation-modulating function compared with BM MSCs *in vitro* and *in vivo*.

Methods

Tissues and blood samples

Research protocols and adherence to donation and ethical consent specific to the tissues used in this study were regulated by the Scottish National Blood Transfusion Service (SNBTS) Research Sample Governance Committee. Non-transplantable LPIs were collected from waste fractions of the pancreatic islet transplant process, following processing of donated organs for clinical transplant [21,22]. These tissues were made available for research following informed written consent, and their use was governed under SNBTS sample governance reference numbers 12-16 and 15-21. Human volunteer-donor buffy coat was used as a source of peripheral blood mononuclear cells (PBMCs) for T-cell responder assays, and chemotaxis assays and were obtained from SNBTS blood processing under sample governance reference number 14-02.

Human platelet lysate

Platelet lysate supplement was produced by repeatedly freezing date-expired human platelet packs, (manufactured in-house by SNBTS) at −80°C for 12 h and thawing at room temperature. The freeze/thaw cycles were repeated 3 times. Upon final thaw, 10 platelet donation packs were pooled and centrifuged at 350 × g before decanting the supernatants as 50-mL aliquots and storing at −40°C.

Culture medium

LPI MSCs were derived, maintained and compared in the following culture media: (i) DMPL-Dulbecco's Modified Eagle's Medium (Thermo Fisher Scientific) supplemented with heparin (Leo Labs) at a final concentration of 21 U/mL, non-essential amino acids 1× (Thermo Fisher Scientific) and 5% human platelet lysate; (ii) SM-StemMACS MSC expansion media kit XF (Miltenyi Biotec Ltd); and (iii) SMPL-StemMACS MSC expansion media kit XF supplemented with 5% human platelet lysate. Unless stated otherwise, studies show LPIs and BM MSCs maintained in SMPL.

Tissue processing and culture initiation

Pancreatic material

Waste LPI fractions were received from the SNBTS islet isolation lab. LPIs were washed once in SMPL medium, centrifuged at 300 × g for 5 min and then cultured at 0.006 mL/cm^2 at 37°C in 5% CO_2 in SMPL medium (e.g., 0.45 mL LPI fraction in a T-75 flask plus 9.5 mL SMPL medium). Explant outgrowth was assessed, and adherent cells were observed migrating from the explanted materials. The medium was carefully exchanged at day 7 and thereafter changed every 3–4 days. Cultures were observed and photographed using an EVOS cell imaging system (Thermo Fisher Scientific). Once the cultures had reached 80–90% confluence, the cells were recovered with a 10-min incubation at 37°C with 0.13 mL/cm^2 TrypLE Select ×1 (Thermo Fisher Scientific). To remove cell debris, the material was passed through a 100-μm cell strainer (Falcon). The cells were counted using a hemocytometer and designated passage 0. These cells were either cryopreserved at 1 × 10^6 per 2-mL cryovial in CryoStor CS10 (Sigma-Aldrich) or re-cultured at a density of 3000 cells/cm^2 in CellBIND flasks (Corning).

Intensification of MSC manufacturing density

Five donations of LPIs were processed at a higher reseeding density of 5000 cells/cm^2 in SM +/− platelet lysate medium at only passage 1 and passage 2.

Bone marrow MSCs

Existing stocks of BM MSC isolates were used in this study for comparison. These cell populations had been previously generated up to passage 3 using standard methods [1].

Medium change/passage

All media were changed twice per week. On reaching 80–90% confluence, cultures were collected as described previously, cell count and yield per flask determined, and reseeded at a density of 3000 cells/cm^2 in CellBIND flasks (Corning). Cells were expanded continually in culture until at least 3 passages of complete cycles of growth to confluence had been achieved after passage 0. Unless

stated otherwise, LPIs and BM MSCs were used at passage 3 throughout this study.

Trilineage differentiation

MSCs were assessed for differentiation capacity using the human mesenchymal stem cell functional identification kit (R&D Systems). This kit contains all necessary differentiation supplements and primary and secondary antibodies required for detection. The mature phenotype of adipocytes, chondrocytes and osteocytes were defined by the binding of antibodies against fatty acid-binding protein 4, aggrecan and osteocalcin, respectively. Primary antibodies were detected using secondary antibodies specific to the primary antibody: NorthernLights 577-conjugated anti-goat (fatty acid-binding protein 4), NorthernLights 557-conjugated donkey anti-mouse (osteocalcin) and NorthernLights 557-conjugated donkey anti-goat (aggrecan). Samples were imaged with a Zeiss epifluorescent microscope and prepared using Zeiss software.

Flow cytometry

Cells were dissociated into a single cell suspension and washed twice in buffer comprising phosphate-buffered saline (PBS), 2 mM ethylenediaminetetraacetic acid and 0.1% human serum albumin (flow buffer). For MSC phenotyping, cells were stained using antibodies at various concentrations (see supplementary Table 1) in a total volume of 100 uL for 15 min at 4°C. Cells were washed 1 time in flow buffer and resuspended in 200 μL of flow buffer for analysis. Voltages were set using fluorescence minus 1 control. A minimum of 10 000 events were collected. Flow cytometry analysis was performed using BD LSRFortessa (BD Biosciences) or MACSQuant and analyzed using FlowJo software (Tree Star).

T-cell suppression assay

T-cell suppression assays were carried out as previously described [14] using ratios of MSCs to PBMCs ranging from 1:2 to 1:16.

Chemotaxis assay

Whole white blood cells were isolated from fresh buffy coat (see supplementary Table 1). MSCs were seeded at 3000 cells/cm^2 in DMPL and grown as a monolayer in 24-well plates (Corning). Once 80% confluence was reached, MSCs were either left unlicensed or licensed. Licensing of MSCs was carried out by incubation of 80% confluent cultures in complete medium supplemented with 10 ng/mL each of interferon gamma, IL-1β and tumor necrosis factor alpha (R&D systems). After 24 h, all wells were washed twice with PBS to remove cytokine, and then 600 μL of fresh DMPL was added to all wells and left for a further 24 h. Next, 5-μm pore inserts (Thermo Fisher Scientific) were placed into the wells on top of the MSCs, and 5.5×10^5 white blood cells in 100 μL DMPL were placed into the inserts. The transwell plate was incubated at 37°C for 3 h before the inserts were carefully removed and discarded. Migrated cells were harvested by collecting the supernatant and washing wells thoroughly with PBS, ensuring a collection of loosely adherent cells. Cells were washed and prepared for flow cytometry using antibodies (see supplementary Table 1). CountBright beads (50 μL), used per the manufacturer's instructions (Life Technologies), were added for cell counting.

Murine air pouch model

A previously established air pouch model was used to assess *in vivo* leukocyte migration induced by transplantation of human MSCs (see supplementary Table 2) [23]. Next, 1×10^6 unlicensed or licensed LPIs or BM MSCs in 1 mL of sterile PBS or sterile PBS alone (control animals) was injected into the air pouch 24 h after the last injection of air. Mice were killed and cells collected as previously described (see supplementary Table 2) after 24 h. Each sample was split into two and stained for 2 separate flow cytometry panels, one to identify mouse innate immune cells and one to identify mouse adaptive immune cells (see supplementary Table 1).

Gene expression

LPIs and BM MSCs were plated at a density of 1×10^5 cells/cm^2 in DMPL. Once MSCs reached 80% confluence, they were licensed as previously described or left as unlicensed controls. Cells were incubated for a further 24 h and then harvested as previously described. Supernatants were frozen at −80°C for Luminex analysis of protein expression (see following). Expression of chemokine, cytokine, chemokine receptor and cytokine receptor genes was assessed using quantitative polymerase chain reaction and human chemokine and receptor RT^2 Profiler polymerase chain reaction array (Qiagen) as previously described [12].

Protein secretion

The 24-h conditioned media from identical samples used for transcript analysis were collected and analyzed using a Luminex 100 analyzer (Bio-Rad Laboratories, Inc) and pre-mixed magnetic multi-analyte kits (R&D Systems) in accordance with the manufacturers' instructions. All reagents and standards were included in the kit and prepared as outlined in the guidelines. Briefly, samples were diluted 2-fold with calibrator diluent (75 μL in 75 μL). Next, 10 μL of the pre-coated microparticle cocktail was added to each well of the 96-well microplates, followed by either 50 μL sample or 50 μL standard, sealed and placed on an orbital shaker (0.12-mm orbit at 800 $\pm$ 50 rpm) for 2 h at room temperature. The plates were washed twice with 100 μL wash buffer per well and then incubated with 50 μL anti-biotin detector antibody per well for 1 h at room temperature on the shaker (0.12-mm orbit at 800 $\pm$ 50 rpm). The plates were washed as previously described, and 50 μL streptavidin-phycoerythrin was added to each well and incubated for 30 min at room temperature. Microparticles were resuspended in 100 μL wash buffer per well and immediately read on the Luminex 100 analyzer (Bio-Rad Laboratories, Inc). Each microparticle bead region was designated and doublets excluded as stated on the certificate of analysis.

Statistics

Graphs and statistical analysis were generated using Prism 6 (GraphPad). Unpaired *t*-tests were used to compare LPI versus BM material and paired *t*-tests utilized when assessing statistical differences within one tissue source. Significant differences are marked on individual figures and represented as $P < 0.05$, $P < 0.01$ and $P < 0.001$.

Results

Establishment of human LPI cultures in GMP-compliant medium

In culture, LPI material initially presented as plastic-adherent islets, identified through positive Dithizone staining and islands of dithizone-negative exocrine tissue (Figure 1A). Adherent, cobblestone-shaped cells grew out from the islets and exocrine tissue as a monolayer, with longer spindle-shaped cells at the outer edges of the monolayer (Figure 1A). Flow cytometric analysis of freshly isolated tissue (day 0) showed that the majority of cells were epithelial cell adhesion molecule (EPCAM) +ve epithelial cells, and no CD90 or CD105 +ve cells were detected (Figure 1B). As cultures matured, EPCAM and MSC marker expression was mutually exclusive, and the prevalence of CD105, CD90 and CD73 cells went from <1% to >90%,

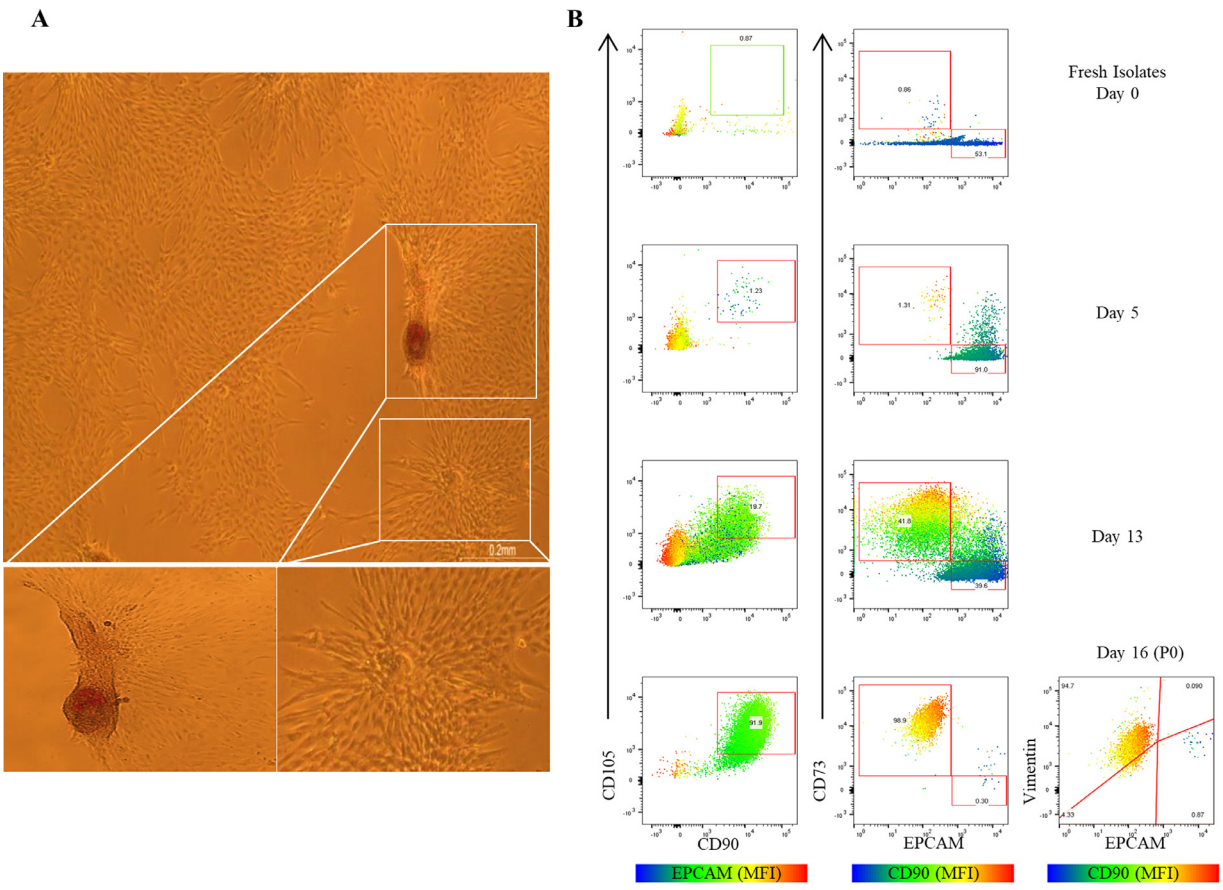

Figure 1. GMP MSC culture derivation from waste LPI fractions of the islet isolation process. (A) Phase contrast micrographs of cellular outgrowth from islands of tissue isolated from LPI fractions. Fourteen days in, culture results in characteristic cobblestone-shaped cells emerging from Dithizone-stained islets and exocrine tissue, forming spindle-shaped MSC-like cells at edges. Scale bar represents 0.2 mm. (B) Three-parameter flow cytometry analysis of MSC and epithelial markers in LPI fraction over time. Flow cytometry plots show an increase in cells expressing CD90, CD105 and CD73 and a decrease in EPCAM-expressing cells over time. An overlay of EPCAM (left column) and CD90 (right columns) shows that MSC and epithelial markers are mutually exclusive. At passage 1, LPI isolates lack EPCAM expression and express CD90, CD105, CD73 and vimentin.

whereas the prevalence of EPCAM-expressing cells went from >50% to <0.3%, over a period of 16 days (Figure 1B). At passage 0, the majority of cells were positive for MSC markers, where 95% of cells were vimentin +ve and <1% were EPCAM +ve (Figure 1B).

LPI-derived cells could be reliably established in GMP-compliant media (DMPL, SM and SMPL), where doubling rate was consistent across all 3 passages (Figure 2A). LPI MSCs grown in SMPL, however, returned significantly higher colony-forming unit fibroblasts at passage 2 and passage 3 compared with DMPL and SM (Figure 2B). There were no differences in colony-forming unit fibroblasts between LPI MSCs and BM MSCs grown in SMPL at any of the 3 passages assessed (Figure 2C). LPI cells established in SMPL displayed a characteristic MSC-like phenotype, through plastic adherence and spindle-shaped morphology, akin to that of BM MSCs grown in SMPL (Figure 3A).

LPI cultures also expressed all the relevant MSC markers, including positive expression of CD73, CD90 and CD105 and no expression of CD45, CD19, CD11b, CD34, CD14 or CD31. This MSC surface marker expression was maintained, and EPCAM expression was consistently lacking through all passages (Figure 3B). LPI-derived cell expression levels of all the aforementioned markers were similar to BM MSCs at passage 3 (Figure 3B). Finally, to confirm that LPI-derived cells were MSCs, LPI cultures were differentiated into the 3 classical lineages: bone, cartilage and adipose. Positive expression of fatty acid-binding protein 4, osteocalcin and aggrecan (Figure 3C) confirmed successful differentiation into all 3 lineages; thus, LPI cultures were considered MSC-like cells and are referred to as LPI MSCs throughout the article.

LPI MSCs and BM MSCs express a range of immunomodulatory and pro-regenerative factors

To understand whether LPI MSCs display therapeutically desirable regenerative and immunomodulatory potential, they were assayed for their transcriptional and protein expression of immune-modulating and pro-regenerative factors, with and without licensing, and compared with BM MSCs at the same passage (Figure 4A,B). Unlicensed LPIs and BM MSCs expressed similar transcriptional patterns of chemoattractant/inflammation-modulating molecules, with the exception of CX3CL1 (fractalkine) and IL-16, which were transcribed at marginally higher levels in the LPI MSCs. Upon licensing, both MSC types uniformly upregulated the inflammatory regulators tumor necrosis factor-inducible gene 6 (TSG-6) and IDO. Patterns in the transcript expression of the pro-angiogenic CXC chemokines were almost identical between LPIs and BM MSCs, where CXCL8 was the most highly transcribed pro-angiogenic gene in LPIs and BM MSCs with or without licensing (Figure 4A).

Various monocyte (CCL2), macrophage (CCL4), dendritic cell (CCL20) and neutrophil chemoattractants (CXCLs 1, 2, 3, 5, 6 and 8) were upregulated upon LPI and BM MSC licensing (Figure 4A). Conditioned media from the same cells used in transcriptional analyses were tested for a selection of pro-angiogenic and chemotactic factors. Secreted proteins from licensed LPIs and BM MSCs closely tracked the transcriptional observations, with high amounts of CCL2, CCL20 and CXCL8 detected in unlicensed MSC supernatants, which were markedly upregulated upon licensing. Vascular endothelial growth factor, a pro-angiogenic factor, was also produced in moderate amounts by resting and licensed MSCs from either source (Figure 4B).

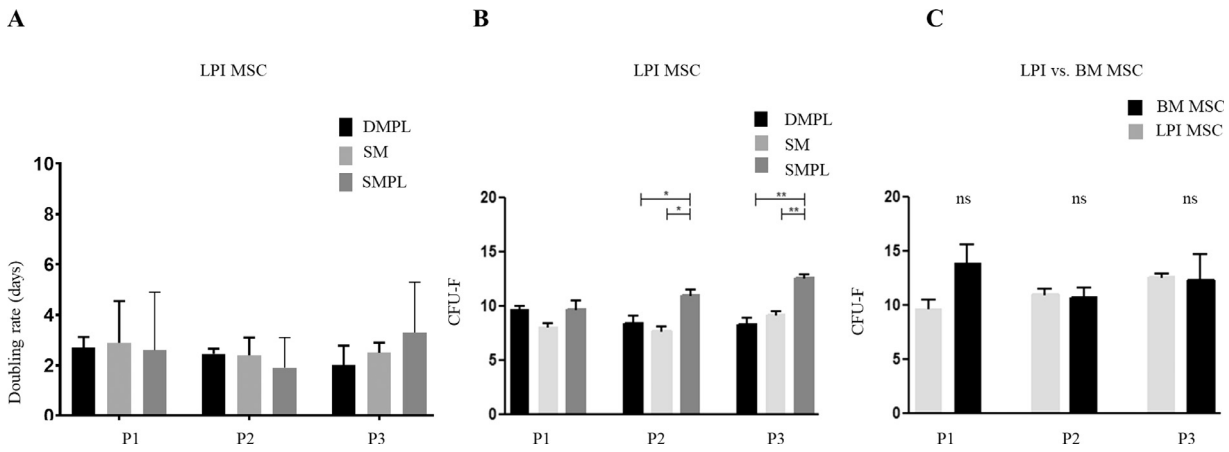

Figure 2. LPI MSC growth characteristics in GMP-compliant media and comparison with BM MSCs. (A) Mean population doubling time for LPI MSC lines in 3 different GMP-compliant media (n = 7). (B) Colony-forming unit scores for LPI MSCs grown in DMPL, SM and SMPL across 3 passages (P1–P3) with numbers of colonies obtained from plating 10 cells/cm^2 in CFU-F (n = 5). (C) Colony-forming unit scores for LPI MSCs versus BM MSCs, both grown in SMPL, across 3 passages (n=9). Data presented as mean ± SD, and significance marked where applicable. $^*P < 0.05$, $^{**}P < 0.01$, $^{***}P < 0.001$. CFU-F, colony-forming unit fibroblast; DMEM, Dulbecco's Modified Eagle's Medium; DMPL, DMEM with 5% platelet lysate; SM, StemMACS; SMPL, StemMACS with 5% platelet lysate; P, passage; SD, standard deviation.

Immune cell attraction profiles of LPIs and BM MSCs are comparable both in vitro *and* in vivo

Chemotaxis assays were utilized to assess whether LPIs and BM MSCs were able to induce migration of immune cells. Unlicensed LPI MSCs differed markedly from BM MSCs in attracting significantly more CD45 +ve cells, specifically neutrophils and monocytes. Upon licensing, both LPIs and BM MSCs attracted neutrophils and monocytes, with little to no attraction of B cells, T cells, natural killer (NK) cells or eosinophils (Figure 5A). LPI MSCs attracted proportionately

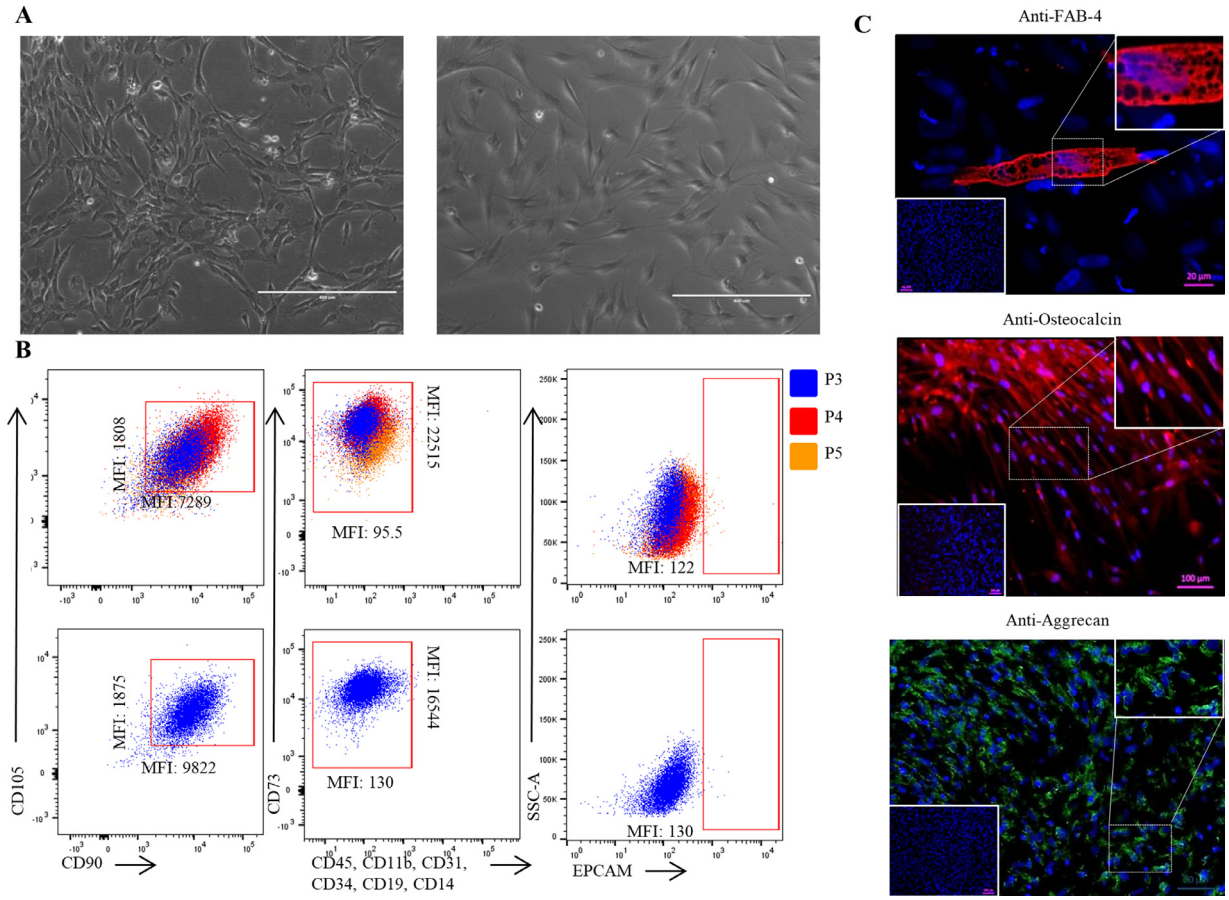

Figure 3. Morphology, surface marker expression and differentiation capability of LPI MSCs. (A) LPI isolate at P1 showing plastic-adherent cells with spindle-like MSC morphology (left) similar to that of BM MSCs at P2 (right) . Scale bar represents 400 μm. (B) Representative phenotypes of LPI MSCs at P3–P5 (top panels) compared with BM MSCs at P3 (bottom panels). LPI MSCs homogeneously express CD90, CD105 and CD73, showing MFI similar to that of BM MSCs, and >99% of LPI MSCs lack expression of CD45, CD11b, CD31, CD34, CD19 and CD14. Lack of EPCAM expression by LPI MSCs is maintained through passage. (C) Fluorescence micrographs of trilineage differentiation of LPI MSCs into adipose, bone and chondrocyte lineages (FAB-4, osteocalcin and aggrecan, respectively). Matched isotype controls shown in bottom left inserts. Scale bar detailed in each picture. Cells grown in SMPL. FAB-4, fatty acid-binding protein 4; MFI, mean fluorescence intensity; P, passage SMPL, StemMACS with 5% platelet lysate.

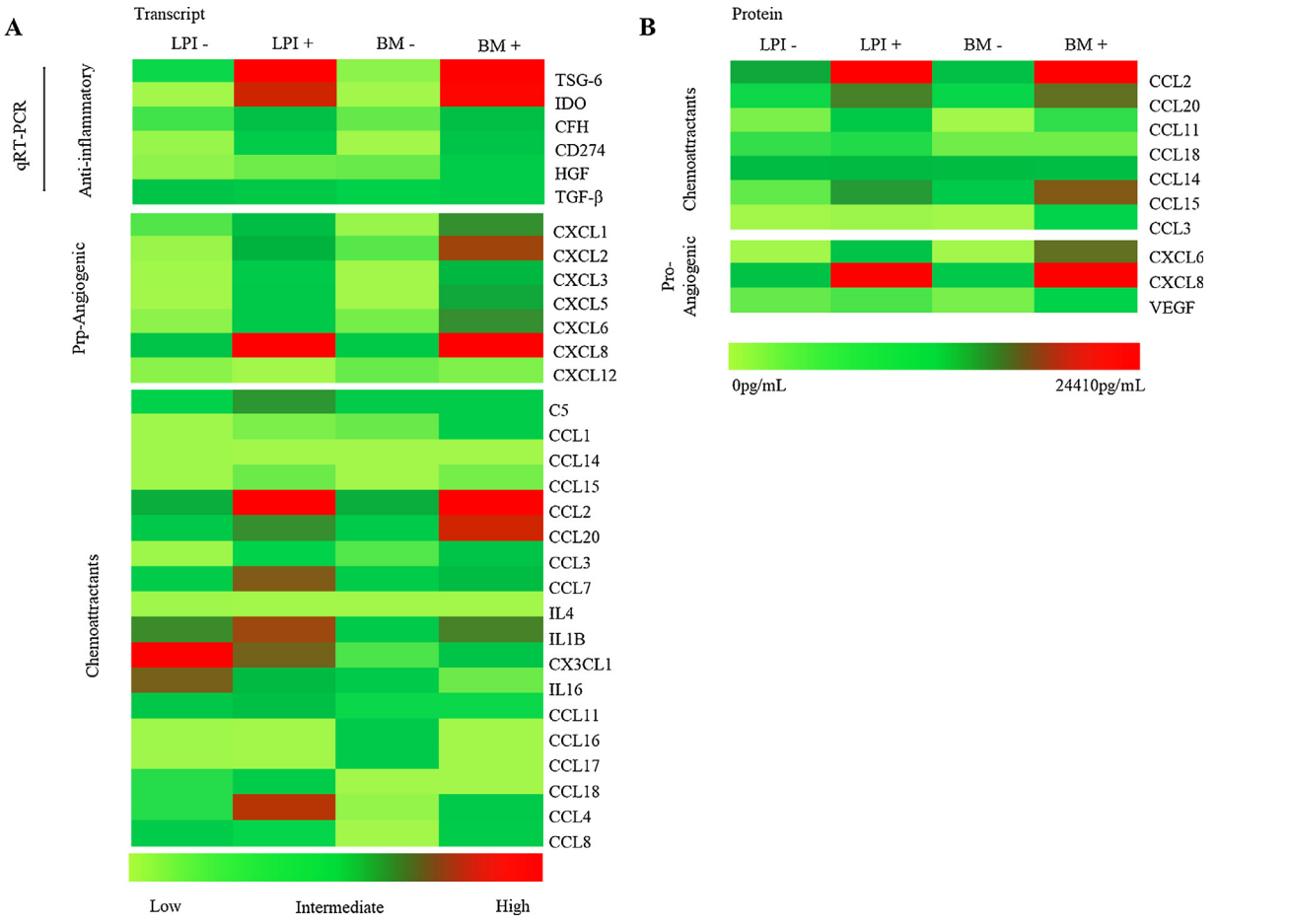

Figure 4. Gene and protein expression of chemoattractant, pro-inflammatory and anti-inflammatory genes in LPIs and BM MSCs. (A) Gene expression by resting and licensed MSCs. The expression of chemoattractant and pro-angiogenic genes by resting (−) and licensed (+) LPIs and BM MSCs (P3) was measured using the RT^2 Profiler PCR array. The expression of anti-inflammatory genes was measured using qRT-PCR as indicated. In each case, the mean $2^{(-\Delta CT)}$ was plotted and heatmaps generated using Heatmapper software. Each group of genes was analyzed separately ($n > 3 < 6$ donors). (B) Mean levels of chemoattractant and pro-angiogenic proteins detected by Luminex assay in 24-h supernatants harvested from the cultures detailed previously. Data represent total concentration of protein minus background levels of each protein found in medium. Analyzed by Heatmapper software as previously noted ($n > 3 < 6$ donors). P, passage; qRT-PCR, quantitative real-time polymerase chain reaction; TSG-6, tumour necrosis factor-inducible gene 6; IDO, indoleamine 2,3-dioxygenase; CFH, complement factor H; CD274, cluster of differentiation 274; HGF, hepatocyte growth factor; TGF-β, transforming growth factor beta; C5, complement component 5; IL4, interleukin 4; IL1β, interleukin-1 beta; IL16, interleukin 16; VEGF, vascular endothelial growth factor.

more monocytes than did BM MSCs, but this did not reach statistical significance.

To establish if observed *in vitro* behaviors of LPIs and BM MSCs persisted *in vivo*, this analysis was extended to a murine air pouch model. In contrast to *in vitro* data, unlicensed LPIs and BM MSCs attracted similar total numbers of all immune cells, with no significant differences detected. As observed *in vitro*, licensing LPIs and BM MSCs resulted in a marked upregulation in the ability of MSCs to induce migration of all immune cells. No significant differences in the total number of immune cells migrating toward licensed LPIs or BM MSCs were observed, with the exception of licensed BM MSCs attracting significantly more NK cells than licensed LPI MSCs. Notably, similar to *in vitro* migration data, neutrophils and monocytes made up the majority of immune cells migrating toward licensed or unlicensed LPIs and BM MSCs; however, the migration of moderate numbers of B cells, NK cells and eosinophils was also observed *in vivo* (Figure 5B).

LPI MSCs are potent suppressors of T-cell proliferation

Suppression of T-cell proliferation by LPIs after activation with the T cell mitogen PHA (Phytohaemagglutinin P) was assessed and compared with BM MSCs. The authors first investigated the capacity of MSCs to suppress T-cell proliferation without licensing. Figure 6A shows representative flow cytometry plots of T cell proliferation under the different conditions. Both LPIs and BM MSCs strongly suppressed T-cell proliferation, at MSC to PBMC ratios of 1:2, and the effect titrated with reducing numbers of MSCs (Figure 6B). Suppression of proliferation by LPI MSCs was significantly higher, at 1:8, than that seen with BM MSCs. Given that strong suppressive effects were seen with unlicensed MSCs, the authors further investigated the role that licensing plays in MSC suppression of T-cell proliferation. Overall, licensing MSCs had no beneficial or detrimental effect on T-cell suppression mediated by MSCs compared with unlicensed MSCs, and no significant differences were observed between LPIs and BM MSCs at any ratio tested (Figure 6C).

GMP-compliant method and density intensification scale up for manufacturing

To scale up for manufacturing, a suitable volume of LPI tissue and subsequent reseeding densities of LPI MSCs had to be determined. Initially, LPI tissue was tested at a density of 0.006 mL/cm^2 or 0.03 mL/cm^2 (1 mL or 5 mL total LPI fraction per T-175 flask in a total volume of 35 mL). Cells were more readily established using the lower seeding density of 0.006 mL/cm^2 (data not shown). Therefore, to model a complete manufacturing process, 1 mL of LPI tissue was seeded into a T-175 flask (0.006 mL/cm^2) and thereafter reseeded at 5000 cells/cm^2.

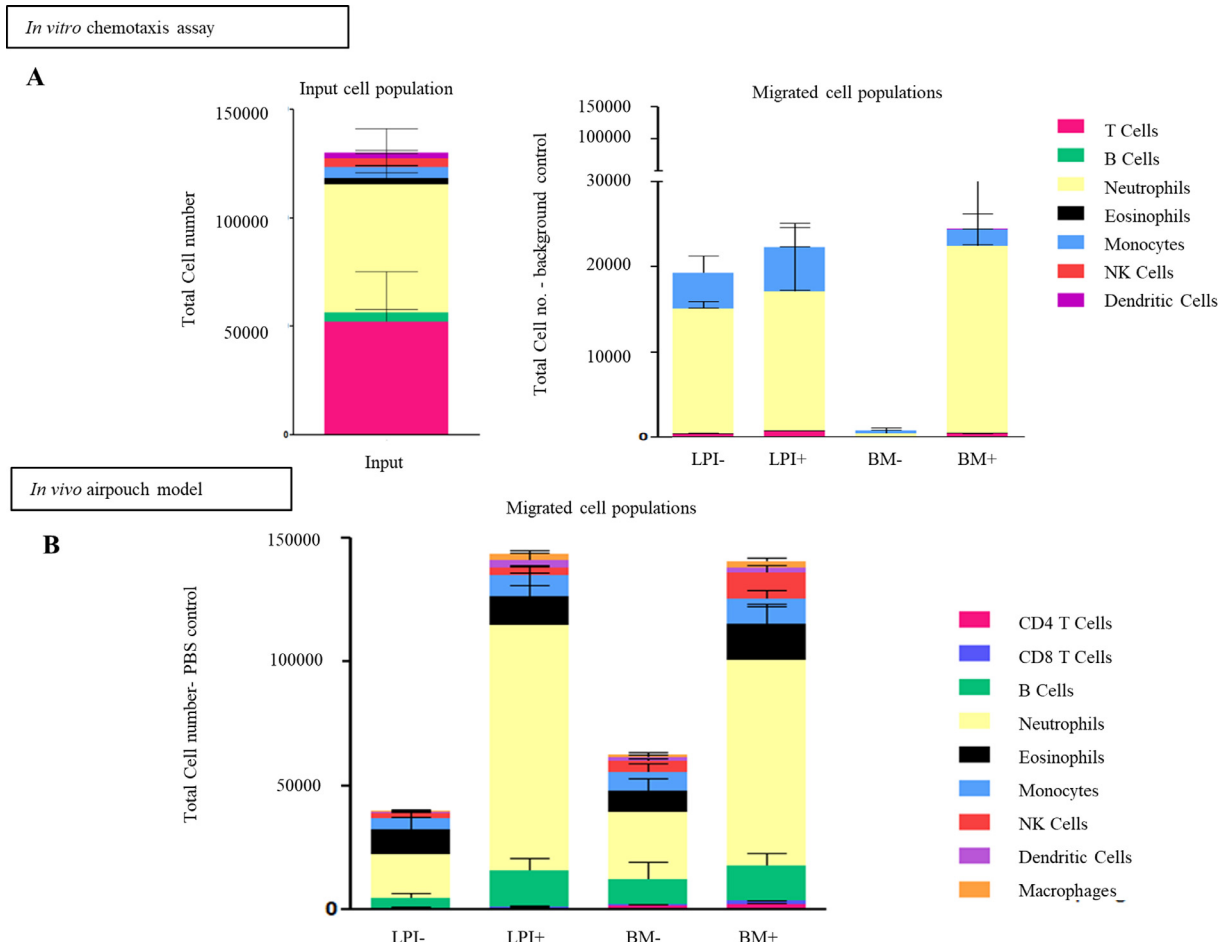

Figure 5. *In vitro* and *in vivo* immune cell attraction of LPI and BM MSCs. (A) *In vitro* chemoattraction of peripheral WBCs. Representative composition of WBCs added to transwell insert at start of chemotaxis experiments. Migration of WBCs to LPI or BM MSCs in the unlicensed (−) or licensed (+) state. Data are presented as mean ± SEM and represent the total number of migrated cells minus the total number of background migrated cells. (B) *In vivo* air pouch model showing the total numbers of migrated immune cells in the air pouch containing licensed or unlicensed LPI or BM MSCs. Data are presented as the total number of each migrated immune cell minus the total numbers in PBS-injected control mice. Stacked bars represent mean ± SEM; n = 2 for each MSC donor and 5 mice per group. WBCs, white blood cells; SEM, standard error of the mean.

The median cell yield at passage 0 was 13×10^6, with a range between 72×10^6 and 4.7×10^6 (Figure 7A). MSCs grown as described previously reached median yields of 5200×10^6 by passage 2 (Figure 7A). As waste tissue from successful islet isolation ranges from 6 mL to 22 mL (Figure 7B), theoretical yields of LPI MSCs at passage 2 could range from $37\,000 \times 10^6$ (6 mL) to $116\,000 \times 10^6$ (22 mL) (Figure 7C). Cells manufactured in this way maintained the CD45 −ve HLA-DR −ve, CD73+, CD90+ CD105+ phenotype (Figure 7D).

Discussion

In this study, the authors have shown that LPI MSC cultures can be easily initiated, and the cells can be expanded to therapeutic scale at low passage. The authors have extensively compared phenotype and function of LPI MSCs with BM MSCs and shown that LPI MSCs share therapeutically relevant characteristics with BM MSCs.

Derivation of LPI-MSCs

MSC-like cells isolated from pancreatic tissue have been described by several groups [19,20]. The authors sought to expand on this work to produce GMP-grade MSC cell populations rather than to reprogram these cells into, for example, beta-like cells. *In vitro*-expanded pancreatic MSC populations may arise from small numbers of resident MSCs or as a result of epithelial-mesenchymal transition (EMT); this has been explored elsewhere [24–27]. The phenotypic changes of LPI isolates described in this study point to EMT as the principal mechanism underlying the derivation of LPI MSC cultures. The authors have shown that freshly isolated LPI tissue lacks cells expressing the mesenchymal markers CD105 and CD90 but is rich in EPCAM +ve cells. Over the 16-day *in vitro* expansion period to reach passage 0, EPCAM +ve cells gradually became positive for CD90 and CD105, followed by a reduction in EPCAM-staining cells to <1% of the total population, which was maintained throughout subsequent passages. At passage 0, over 91% of cells expressed the definitive mesenchymal marker vimentin. From passage 1 onward, MSCs expressed CD105, CD90 and CD73. It is therefore most likely that the LPI MSC manufacturing processes described in this study produced isolates of culture-induced MSC-like cells as a result of *in vitro* EMT, although involvement of small populations of precursors cannot be entirely ruled out.

Function and phenotype

International Society for Cell & Gene Therapy criteria for definition of MSCs [28] have underpinned all recent MSC research, and the LPI MSCs generated in this study met all of these criteria. Phenotype alone does not reveal whether MSCs from different sources or MSCs cultured using different methods have equal therapeutic capacity. The authors recently reported that umbilical cord-derived MSCs, when co-transplanted with islets into diabetic mice, have a greater benefit on glycemic control than identically cultured adipose-derived

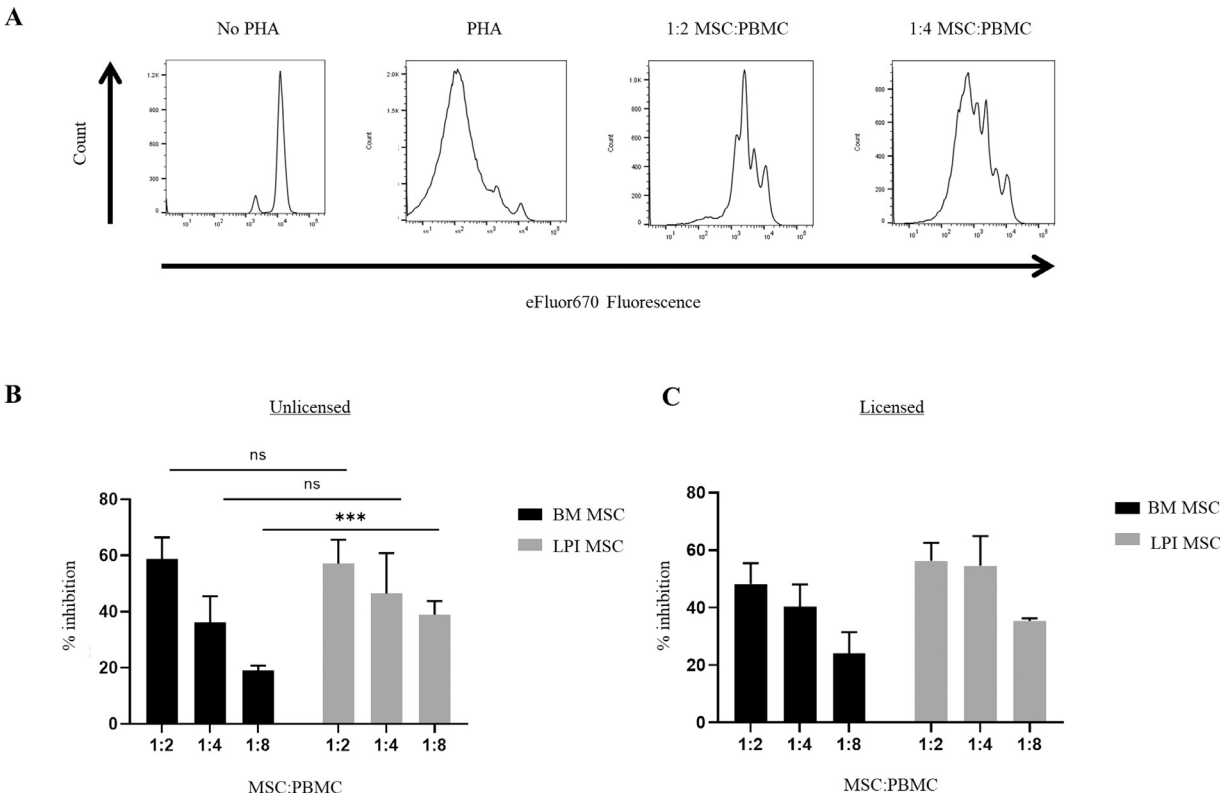

Figure 6. Inhibition of T-cell proliferation and requirement for IFN-γ licensing. (A) Representative dye dilution results measuring inhibition of T-cell proliferation by LPI or BM MSCs. Cells were grown in SMPL, assayed at P3 and cultured with Ef670-stained PBMCs. Ratios are PBMC:MSC at outset of culture. (B) Comparative inhibition of T-cell proliferation by unlicensed LPI or BM MSCs. Both MSC types inhibit proliferation, and the effects titrate with reducing MSC numbers. Mean of 3 different LPI and 4 different BM lines grown in SMPL. Ratios are PBMC:MSC. (C) Comparative inhibition of T-cell proliferation by licensed LPI or BM MSCs. Mean of 3 different LPI and 4 different BM lines grown in SMPL. Ratios are PBMC:MSC. IFN-γ, interferon gamma; P, passage; PHA, Phytohaemagglutinin P; PBMC,peripheral blood mononuclear cells: SMPL, StemMACS with 5% platelet lysate.

MSCs, and that these MSC isolates differ widely in expression of genes important in immune response and angiogenesis [14]. Here the authors took a similar standardized approach in the analysis to systematically compare LPI MSCs with BM MSCs to ensure that they share clinically applicable characteristics beyond basic phenotyping. Transcriptional analysis of more than 30 genes highlighted that LPI MSCs express immunomodulatory, pro-angiogenic and chemotactic factors similar to BM MSCs. BM and LPI MSCs responded to licensing with upregulation of a number of genes, including the immune modulators TSG-6 [29] and IDO [30], the pro-angiogenic and neutrophil chemoattractants CXCL2 and CXCL8 [31,32] and the monocyte chemoattractant (and pro-angiogenic) CCL2 [33].

The authors have shown that these transcribed genes translate into *in vitro* and *in vivo* activity of MSCs, with similar patterns in protein secretion between LPI and BM MSCs. *In vitro*, strong chemoattraction of myeloid cells was a function of licensed LPI and BM MSCs. *In vivo*, unlicensed BM and LPI MSCs both induced infiltration of neutrophils and monocytes into the injection site. This function was greatly amplified when MSCs were licensed before injection. Recruitment of inflammatory cells may be an unexpected function of cells with proven anti-inflammatory properties; however, recruitment of circulating monocytes has been shown to be critical for microvascular growth [34]. Moreover, neutrophil recruitment has been shown to be necessary for blood vessel formation in an *in vivo* angiogenesis model [35]. The chemoattraction of immune cells toward MSCs likely serves more than one purpose, extending beyond angiogenesis to immunomodulation of these attracted immune cells, presumably altering the inflammatory environment. Here the authors have shown that BM and LPI MSCs not only attract similar types and numbers of immune cells but also express similar patterns of the immunomodulatory genes TSG-6, IDO and TGF-β while exerting similar capacity to suppress T-cell proliferation. The ability of MSCs to attract immune cells and subsequently immunosuppress them is an important therapeutic mode of action that has been demonstrated in a model of GVHD [36]. Treatment of GVHD is an area where LPI MSCs may offer an advantage over BM MSCs, as LPI MSCs suppressed T-cell proliferation at lower ratios of T cells to MSCs and attracted more myeloid cells in an unlicensed state. LPI MSCs could also potentially be used in islet transplant recipients, as MSCs have been shown to enhance engraftment and function in experimental models [14]. Patients routinely receive 2 islet grafts [21]; hence, MSCs could be generated from the LPIs of the first transplant and used subsequently as MHC-matched accessory cells to support the second graft, with potentially reduced immune sensitization compared with third-party MSCs.

Manufacture of LPI MSCs

Extending the applications of a donated pancreas beyond high-purity islet transplantation to involve the manufacture of MSCs from the LPI fraction would extend clinical application of the donated organ to potentially treat many patients. Recent registry data indicate >2600 donated pancreata for islet processing (North America, Europe and Australia) [37] over a 10-year period ending 2015. LPI fractions are therefore routinely available from transplant centers and should be readily available for distribution to manufacturing centers. LPI-MSCs grow rapidly in xenogeneic-free medium; a single T-175 flask initially seeded with 1 mL of LPIs can generate 5.2×10^9 cells after 2 *in vitro* passages, with theoretical yields from a single LPI fraction of 31.7×10^9 to 116×10^9. This would result in sufficient MSCs to manufacture 356–1303 doses (based on 1×10^6 cells/kg and a patient weighing 89 kg). This compares favorably with projected manufacturing yields for BM MSCs

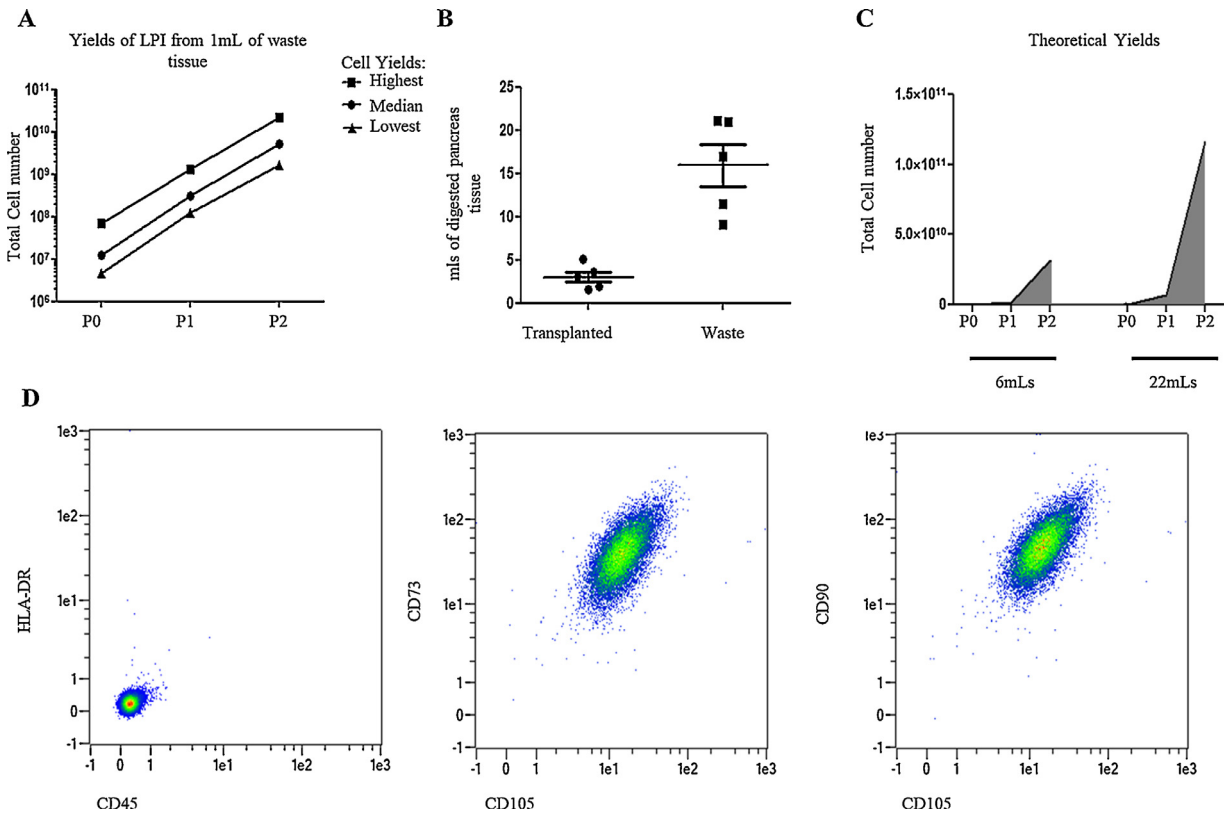

Figure 7. Intensification of manufacturing with GMP reagents. (A) Total cell yields from 1 mL of LPI tissue from P0 to P1 in GMP-compliant medium. (B) Total milliliters of transplanted tissue versus waste tissue in the GMP islet isolation process. (C) Predicted cell yields from the lowest volume of waste tissue (6 mL) over 2 passages and the highest volume of waste tissue (22 mL) over 2 passages. (D) Flow cytometric analysis of LPI MSCs grown using the intensified method, demonstrating negativity for hematopoietic markers and homogeneous expression of CD73, CD90 and CD105. SMPL medium passage 3. GMP, good manufacturing practice; P, passage; SMPL, StemMACS with 5% platelet lysate.

under GMP conditions using a whole bone marrow donation (20–37 mL) and standard culture vessels: 6.6×10^9 at passage 2 and up to 6.3×10^9 at passage 1 [3,6]. Manufacture of MSCs, irrespective of source, at this scale would become impractical using standard culture vessels and would benefit from the use of bioreactors, not necessarily to increase yield—although this is not guaranteed [34]—but for ease of handling and speed of processing. Manufacturing on a very large scale may well not be required in a single center, as a single LPI fraction from a donated pancreas could support manufacturing in a number of different centers. Samples from a single isolation, in simple storage media, are routinely distributed fresh from the SNBTS islet isolation lab around the UK to multiple centers, subject to appropriate consent.

In summary, the authors have demonstrated that MSCs derived from LPI fractions exhibit many of the ideal immune-responsive and pro-regenerative functions of MSCs *in vitro* and *in vivo*. These cells are readily expanded from donated clinical-grade material that is currently an unused byproduct of islet isolation, and the authors have demonstrated their successful manufacture using fully GMP-compliant materials to therapeutic dose at low passage. Further studies will be required to determine the therapeutic potency of this novel MSC population.

Funding

This study was supported in part by the Scottish Chief Scientist Office (grant nos. ETM/325 and TCS/17/31 to JC and SF, principal investigators). KLT was in receipt of a Scottish National Blood Transfusion Service-funded PhD studentship awarded to GJG and JDMC. Work in GJG's lab is supported by a Wellcome Investigator Award and an MRC Programme grant. The Edinburgh Islet Isolation Laboratory is supported by the NHS National Services Division.

Declaration of Competing Interest

The authors have no commercial, proprietary or financial interest in the products or companies described in this article.

Author Contributions

Conception and design of the study: DC, JCM, NWAM, JJC, GJG, MLT, SF and JDMC. Acquisition of data: KLT, DC, KS, LB, NC-G, KDH, CJK, CCW, NWAM and JDMC. Analysis and interpretation of data: KLT, DC, JCM, KS, LB, NC-G, KDH, CJK, GJG, SF and JDMC. Drafting or revising the manuscript: KLT, KDH, GJG and JDMC. All authors have approved the final article.

Acknowledgments

The authors gratefully acknowledge the support of the Edinburgh Islet Isolation Laboratory. The authors thank Dick Drake, Anne Mackie and Paul Hopkinson for technical support. The authors also thank the blood donors, organ donors and their families. Without their support, this study would not have been possible.

Supplementary materials

Supplementary material associated with this article can be found in the online version at doi:10.1016/j.jcyt.2020.07.010.

References

[1] Galipeau J, Sensébé L. Mesenchymal Stromal Cells: Clinical Challenges and Therapeutic Opportunities. Cell Stem Cell 2018;22(6):824–833.
[2] v1. https://clinicaltrials.gov/; 2019. [Accessed 10 July 2020].
[3] Laitinen A, Oja S, Kilpinen L, Kaartinen T, Moller J, Laitinen S, et al. A robust and reproducible animal serum-free culture method for clinical-grade bone marrow-derived mesenchymal stromal cells. Cytotechnology 2016;68(4):891–906.
[4] Bruna F, Contador D, Conget P, Erranz B, Sossa CL, Arango-Rodriguez ML. Regenerative Potential of Mesenchymal Stromal Cells: Age-Related Changes. Stem cells international 2016;2016:1461648.
[5] Ganguly P, El-Jawhari JJ, Burska AN, Ponchel F, Giannoudis PV, Jones EA. The Analysis of *In Vivo* Aging in Human Bone Marrow Mesenchymal Stromal Cells Using Colony-Forming Unit-Fibroblast Assay and the CD45(low)CD271(+) Phenotype. Stem cells international 2019;2019:5197983.
[6] Fekete N, Rojewski MT, Furst D, Kreja L, Ignatius A, Dausend J, et al. GMP-compliant isolation and large-scale expansion of bone marrow-derived MSC. PloS one 2012;7(8):e43255.
[7] von Bahr L, Sundberg B, Lonnies L, Sander B, Karbach H, Hagglund H, et al. Long-term complications, immunologic effects, and role of passage for outcome in mesenchymal stromal cell therapy. Biology of blood and marrow transplantation: journal of the American Society for Blood and Marrow Transplantation 2012;18(4):557–64.
[8] James AW, Zara JN, Corselli M, Askarinam A, Zhou AM, Hourfar A, et al. An abundant perivascular source of stem cells for bone tissue engineering. Stem cells translational medicine 2012;1(9):673–84.
[9] Sarugaser R, Ennis J, Stanford WL, Davies JE. Isolation, propagation, and characterization of human umbilical cord perivascular cells (HUCPVCs). Methods in molecular biology (Clifton, NJ) 2009;482:269–79.
[10] West CC, Hardy WR, Murray IR, James AW, Corselli M, Pang S, et al. Prospective purification of perivascular presumptive mesenchymal stem cells from human adipose tissue: process optimization and cell population metrics across a large cohort of diverse demographics. Stem cell research & therapy 2016;7:47.
[11] Kehl D, Generali M, Mallone A, Heller M, Uldry AC, Cheng P, et al. Proteomic analysis of human mesenchymal stromal cell secretomes: a systematic comparison of the angiogenic potential. NPJ Regenerative medicine 2019;4:8.
[12] Merckx G, Hosseinkhani B, Kuypers S, Deville S, Irobi J, Nelissen I, et al. Angiogenic Effects of Human Dental Pulp and Bone Marrow-Derived Mesenchymal Stromal Cells and their Extracellular Vesicles. Cells 2020;9(2):312.
[13] Balasubramanian S, Venugopal P, Sundarraj S, Zakaria Z, Majumdar AS, Ta M. Comparison of chemokine and receptor gene expression between Wharton's jelly and bone marrow-derived mesenchymal stromal cells. Cytotherapy 2012;14(1):26–33.
[14] Forbes S, Bond AR, Thirlwell KL, Burgoyne P, Samuel K, Noble J, et al. Human umbilical cord perivascular cells improve human pancreatic islet transplant function by increasing vascularization. Science translational medicine 2020;12(526):eaan5907.
[15] Sotiropoulou PA, Perez SA, Gritzapis AD, Baxevanis CN, Papamichail M. Interactions between human mesenchymal stem cells and natural killer cells. Stem cells (Dayton, Ohio) 2006;24(1):74–85.
[16] Cui R, Rekasi H, Hepner-Schefczyk M, Fessmann K, Petri RM, Bruderek K, et al. Human mesenchymal stromal/stem cells acquire immunostimulatory capacity upon cross-talk with natural killer cells and might improve the NK cell function of immunocompromised patients. Stem cell research & therapy 2016;7(1):88.
[17] Noronha NC, Mizukami A, Caliari-Oliveira C, Cominal JG, Rocha JLM, Covas DT, et al. Priming approaches to improve the efficacy of mesenchymal stromal cell-based therapies. Stem cell research & therapy 2019;10(1):131.
[18] Polchert D, Sobinsky J, Douglas G, Kidd M, Moadsiri A, Reina E, et al. IFN-gamma activation of mesenchymal stem cells for treatment and prevention of graft versus host disease. European journal of immunology 2008;38(6):1745–55.
[19] Seeberger KL, Dufour JM, Shapiro AM, Lakey JR, Rajotte RV, Korbutt GS. Expansion of mesenchymal stem cells from human pancreatic ductal epithelium. Laboratory investigation; a journal of technical methods and pathology 2006;86(2):141–53.
[20] Khiatah B, Qi M, Du W, K TC, van Megen KM, Perez RG, et al. Intra-pancreatic tissue-derived mesenchymal stromal cells: a promising therapeutic potential with anti-inflammatory and pro-angiogenic profiles. Stem cell research & therapy 2019;10(1):322.
[21] Forbes S, McGowan NW, Duncan K, Anderson D, Barclay J, Mitchell D, et al. Islet transplantation from a nationally funded UK centre reaches socially deprived groups and improves metabolic outcomes. Diabetologia 2015;58(6):1300–8.
[22] Shapiro AM, Lakey JR, Ryan EA, Korbutt GS, Toth E, Warnock GL, et al. Islet transplantation in seven patients with type 1 diabetes mellitus using a glucocorticoid-free immunosuppressive regimen. The New England journal of medicine 2000;343(4):230–8.
[23] Dyer DP, Medina-Ruiz L, Bartolini R, Schuette F, Hughes CE, Pallas K, et al. Chemokine receptor redundancy and specificity are context dependent. Immunity 2019;50(2):378–89.
[24] Lee S, Jeong S, Lee C, Oh J, Kim SC. Mesenchymal Stem Cells Derived from Human Exocrine Pancreas Spontaneously Express Pancreas Progenitor-Cell Markers in a Cell-Passage-Dependent Manner. Stem cells international 2016;2016:2142646.
[25] Sordi V, Melzi R, Mercalli A, Formicola R, Doglioni C, Tiboni F, et al. Mesenchymal cells appearing in pancreatic tissue culture are bone marrow-derived stem cells with the capacity to improve transplanted islet function. Stem cells (Dayton, Ohio) 2010;28(1):140–51.
[26] Chase LG, Ulloa-Montoya F, Kidder BL, Verfaillie CM. Islet-derived fibroblast-like cells are not derived via epithelial-mesenchymal transition from Pdx-1 or insulin-positive cells. Diabetes 2007;56(1):3–7.
[27] Gershengorn MC, Hardikar AA, Wei C, Geras-Raaka E, Marcus-Samuels B, Raaka BM. Epithelial-to-mesenchymal transition generates proliferative human islet precursor cells. Science 2004;306(5705):2261–4.
[28] Cook G, Campbell JD, Carr CE, Boyd KS, Franklin IM. Transforming growth factor beta from multiple myeloma cells inhibits proliferation and IL-2 responsiveness in T lymphocytes. Journal of leukocyte biology 1999;66(6):981–8.
[29] Campbell JD, Cook G, Robertson SE, Fraser A, Boyd KS, Gracie JA, et al. Suppression of IL-2-induced T cell proliferation and phosphorylation of STAT3 and STAT5 by tumor-derived TGF beta is reversed by IL-15. Journal of immunology 2001;167(1):553–61.
[30] Dominici M, Le Blanc K, Mueller I, Slaper-Cortenbach I, Marini F, Krause D, et al. Minimal criteria for defining multipotent mesenchymal stromal cells. The International Society for Cellular Therapy position statement. Cytotherapy. 2006;8(4):315–7.
[31] Yun YI, Park SY, Lee HJ, Ko JH, Kim MK, Wee WR, et al. Comparison of the anti-inflammatory effects of induced pluripotent stem cell-derived and bone marrow-derived mesenchymal stromal cells in a murine model of corneal injury. Cytotherapy 2017;19(1):28–35.
[32] Keane MP, Belperio JA, Moore TA, Moore BB, Arenberg DA, Smith RE, et al. Neutralization of the CXC chemokine, macrophage inflammatory protein-2, attenuates bleomycin-induced pulmonary fibrosis. Journal of immunology 1999;162(9):5511–8.
[33] Corliss BA, Azimi MS, Munson JM, Peirce SM, Murfee WL. Macrophages: An Inflammatory Link Between Angiogenesis and Lymphangiogenesis. Microcirculation 2016;23(2):95–121.
[34] Massena S, Christoffersson G, Vagesjo E, Seignez C, Gustafsson K, Binet F, et al. Identification and characterization of VEGF-A-responsive neutrophils expressing CD49d, VEGFR1, and CXCR4 in mice and humans. Blood 2015;126(17):2016–26.
[35] Galleu A, Riffo-Vasquez Y, Trento C, Lomas C, Dolcetti L, Cheung TS, et al. Apoptosis in mesenchymal stromal cells induces *in vivo* recipient-mediated immunomodulation. Science translational medicine 2017;9(416):eaam7828.
[36] Mizukami A, Pereira Chilima TD, Orellana MD, Neto MA, Covas DT, Farid SS, Swiech K. Technologies for large-scale umbilical cord-derived MSC expansion: experimental performance and cost of goods analysis. Biochemical Engineering Journal 2018;135:36–48.
[37] v1. https://citregistry.org/; 2020. [Accessed 10 July 2020].